LAPPEENRANTA UNIVERSITY OF TECHNOLOGY
Faculty of Technology
Department of Chemical Technology

Master of Science Thesis

CALCINATION OF ALUMINUM HYDROXIDE OVER PRESSURE AND RESIDENCE TIME

The subject of this thesis has been approved by the Department of Chemical Technology on 17.6.2008.

Examiners: Prof. Dr. Ilkka Turunen
M.Sc. Michael Missalla

Instructor: M.Sc. Michael Missalla

Two versions of this thesis have been made, a confidential (until 8/2018) and a public version. This copy is the public version.

In Lappeenranta on 18.8.2008

Sameli Hakola
Poukantie 3
04400 Järvenpää
Finland

+358 44 5653 194

ACKNOWLEDGEMENTS

First of all, I would like to thank Professor Ilkka Turunen from Lappeenranta University of Technology as well as Dr. Nikola Anastasijevic from Outotec GmbH for granting me the opportunity to do my thesis at Outotec's R&D Center in Frankfurt. I would also like to thank my supervisors, Mr. Michael Missalla and Mr. Peter Sturm for their advice and contribution to my work.

Other people that I would like to acknowledge are Mr. Andreas Spies, Ms. Viola Nischan, Mr. Aderito Martinho da Silva and last but most certainly not least, Dr. Alpaydin Saatci. Furthermore, I would like to thank my new friends here in Frankfurt whom have supported me during my work: Sebastian Pinke, Fernando Parada Torres, Dimitri Melnikowitsch and Christian Zimmerman.

I also thank my parents, Hannele and Jyrki, for their support and finally my girlfriend Anni-Mari.

In Frankfurt am Main on Wednesday the 6th of August 2008.

Sameli Hakola

ABSTRACT

Lappeenranta University of Technology
Faculty of Technology
Department of Chemical Technology
Sameli Hakola

CALCINATION OF ALUMINUM HYDROXIDE OVER PRESSURE AND RESIDENCE TIME

Master of Science Thesis

2008

90 pages, 32 figures and 14 tables, 2 appendix

Examiners: Prof. Dr. Ilkka Turunen

M. Sc. Michael Missalla

Keywords: Calcination, Aluminum hydroxide, Alumina

This work investigates the possible effect of pressure and residence time to the reaction of aluminum hydroxide into aluminum oxide. Various pressurized conditions are used as well as the help of various residence times. The aim is to increase the conversion of the reaction with the use of different pressures and residence times. The tests were performed with a laboratory scale fluidized bed reactor at the Outotec R&D Center in Frankfurt. Additional test work such as particle size analysis and differential thermal analysis were also carried out. Some calcined samples were also characterized with X-ray diffraction at the University of Auckland to obtain a reaction pathway when using pressurized conditions. All of the results are then compared with previous results.

TIIVISTELMÄ

Lappeenrannan Teknillinen Yliopisto
Teknillinen tiedekunta
Kemiantekniikan osasto
Sameli Hakola

ALUMIINIHYDROKSIDIN PAINEISTETTU KALSINOINTI USEILLA VIIPYMÄAJOILLA

Diplomityö

2008

90 sivua, 32 kuvaa ja 14 taulukkoa, 2 liitettä

Tarkastajat: Professori TkT Ilkka Turunen

DI Michael Missalla

Hakusanat: Kalsinointi, Alumiinihydroksidi, Alumiinioksidi

Tässä työssä tutkittiin paineen sekä viipymäajan vaikutusta alumiinihydroksidin kalsinoinnissa alumiinioksidiksi. Työssä käytettiin useita paineistettuja olosuhteita kuten myös useita eri viipymäaikoja. Työn tavoite oli kasvattaa reaktion konversiota käyttäen näitä kahta parametria hyväksi. Kokeet suoritettiin käyttäen laboratoriomittakaavassa olevaa leijupetireaktoria Outotecin tutkimuskeskuksessa Frankfurtissa. Kokeita, kuten partikkelikokoanalyysejä sekä differentiaalisia termisiä analyysejä suoritettiin varsinaisten kokeiden lisäksi. Osa kalsinoiduista näytteistä karakterisoitiin käyttäen röntgendiffraktiota Aucklandin yliopistossa. Tämän tarkoituksena oli tutkia reaktion kulkua raaka-aineesta tuoteeksi. Kokeiden tuloksia verrattiin lopuksi aikaisempiin tuloksiin.

NOMENCLATURE

Latin Symbols

d_p	Particle size	[m]
k	Reaction rate coefficient	[-]
L	Length of bed	[m]
LOI	Loss On Ignition	[%]
m_1	Mass of empty crucible	[g]
m_2	Mass of empty crucible and sample	[g]
m_3	Mass of empty crucible and dries sample	[g]
m_4	Mass of empty crucible and ignited sample	[g]
MOI	Moisture On Ignition	[%]
$P_{1,2}$	Pressure of the old and new gas	[Pa]
$P_{H_2O(g)}$	Partial pressure of steam	[Pa]
$P^{Eq.}$	Equilibrium pressure	[Pa]
$P^{Prev.}$	Prevalent steam partial pressure	[Pa]
SSA	Specific surface area	[m^2/g]
$T_{1,2}$	New and old gas temperatures	[K]
U_{mf}	Minimum fluidization velocity	[m/s]
U_{mb}	Minimum bubbling velocity	[m/s]
$v_{calcination}$	rate of calcination	[-]
$\dot{V}_{H_2O(g)}$	Volume flow of steam	[L/min]
$\dot{V}_{new,old}$	New and old volume flow	[m^3/h]

Greek symbols

ρ_f	Fluid density	[kg/m^3]
ε	Bed voidage factor	[-]
φ_s	Particle shape factor	[-]
ρ_p	Particle density	[kg/m^3]
$\rho_{1,2}$	Densities of new and old gases	[kg/m^3]

TABLE OF CONTENTS

1 INTRODUCTION

Calcination is the final step of the Bayer process where aluminum trihydroxide is produced from bauxite. After calcination, alumina is sent to a smelter where pure aluminum is produced. The Bayer process was originally invented by an Austrian chemist named Karl Joseph Bayer in 1888. The process comprises steps such as raw material preparation, digestion, insoluble bauxite residue separation, precipitation and finally calcination. In raw material preparation, the bauxite ore is ground as a slurry into a state where the particle size is less than 0,15 cm. The main goal of digestion is the extraction of Al_2O_3 out of bauxite. Here, the selective extraction of aluminum hydroxides from the impurities is done by dissolving bauxite in sodium hydroxide (caustic soda). The insoluble bauxite residue is separated via clarifiers and thickeners. Before calcination, $Al(OH)_3$ is recovered from the solution via precipitation. (Hudson *et al*[1], 2000)

As the world continuously moves towards rising crude oil and natural gas prices companies are faced with an important question: how can we make our process more efficient in terms of energy consumption? Naturally, indirect energy saving via heat recovery from hot product and waste gas streams have to be made use of but the real question is how to make the actual process more energy efficient. Currently, when the energy needed for the production of alumina has reached a fairly low amount the process parameters have to be thought through. Some changes in them might lower the need for energy even further. These changes can possibly be process parameters such as residence time and the use of pressure.

This thesis was done in 2008 at the Outotec GmbH R&D Center in Frankfurt am Main. The first objective of this thesis was to investigate the possibility of energy saving by varying two process parameters: pressure and residence time with many different temperatures. The effect of pressure is investigated due to the fact that previous results have implied that pressure would have a promoting effect to calcination. It could possibly be a factor in lowering the energy consumption during calcination.

The second goal is to investigate the reaction pathway of the decomposition of aluminum trihydroxide into its stable final. The reason for this is to determine

whether pressure has an effect to the route of the calcination reaction. this is done via characterizing samples prepared under pressurized conditions. Thirdly, few particle size analysis' are investigated for the possible effect of pressure to the mean particle size. Here, previous results have shown that particles shrink during calcination. Finally, an operating procedure for the calcination apparatus is given to aid future researchers.

2 ALUMINUM OXIDE

Alumina is the general name for aluminum oxide. It is a white powder and best known for its hardness and electric resistance. The biggest producer country of alumina in the world is Australia which manufactured 16 271 000 tons in 2001. Furthermore, the biggest consumer of alumina is the aluminum industry and the bulk price of alumina is roughly 140 $/ton.

2.1 Raw material, bauxite

The main raw materials are bauxite ores which are sedimentary rocks containing gibbsite, boehmite or diaspore. Mainly the composition of bauxite is a combination of aluminum oxide, iron oxide as well as titanium and silicon dioxides. Gibbsite is the most attractive type. This is, because boehmite and diaspore need more harsh conditions (higher temperatures) in the Bayer process to dissolute. Therefore, as long as there is an abundance of bauxite rich of gibbsite, it will maintain its attractiveness compared to boehmite and diaspore. (Hudson *et al*[1] 2000)

The major price and quality determining factor of bauxite ore is the amount of reactive silica, silicon dioxide. Sodium aluminate reacts with these aluminosilicates, SiO_2, forming an insoluble sodium aluminum silicates during digest, a part of the Bayer process. This leads to the loss of sodium hydroxide and extractable alumina. Australia is the home of the largest reserves of bauxite ($7\ 900\ 000 \cdot 10^3$ t). Brazil has the second largest reserves ($2\ 900\ 000 \cdot 10^3$ t) and Jamaica and China share the third place with reserves of $2\ 000\ 000 \cdot 10^3$ t each. (Hudson *et al*[1], 2000)

2.2 Forms of aluminum hydroxide

Aluminum hydroxides are generally classified as shown in figure 1. The main categories are crystalline and gelatinous forms. Basically, the crystalline forms

consist of the three trihydroxides, $Al(OH)_3$: gibbsite, nordstrandite and bayerite. Furthermore, there are two modifications of aluminum oxide hydroxide, AlO(OH): boehmite and diaspore. The two gelatinous forms of aluminum hydroxide are X-ray indifferent aluminum hydroxide and pseudoboehmite. (Hudson *et al*[1], 2000)

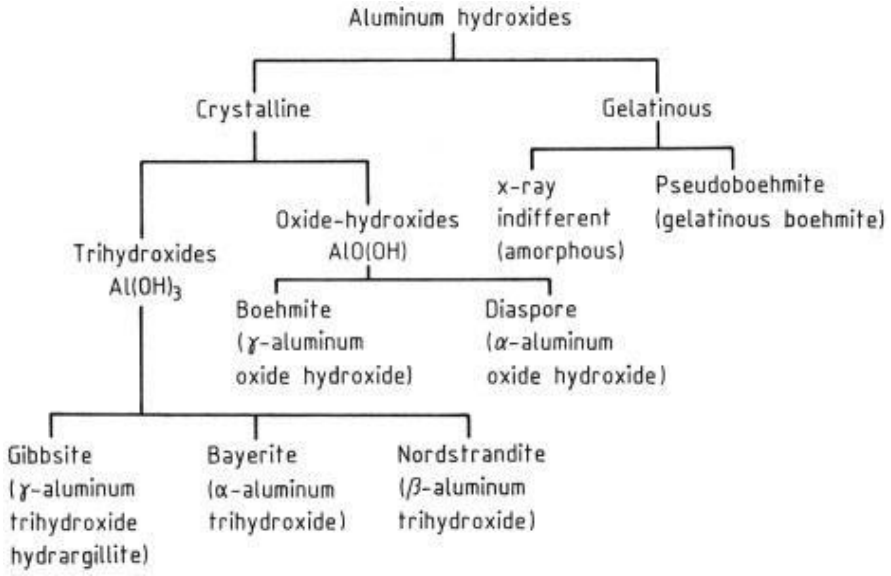

Figure 1. The classification of aluminum hydroxides. (Adapted from Hudson *et al*[1], 2000)

Bayerite is not normally found in nature. Actually, there are only a few places in the world where natural bayerite has been reported. The abundant aluminum hydroxides in nature are gibbsite, boehmite and diaspore. For the purposes of this thesis, the key aluminous materials are gibbsite and boehmite. Also, gamma alumina (γ-Al_2O_3) and alpha alumina (α-Al_2O_3), products of gibbsite when it is treated thermally, are also important (see chapter 2, Calcination). (Hudson *et al*[1], 2000)

The nomenclature related to the aluminum hydroxides is fairly unsystematic. Bayerite, gibbsite and nordstrandite are trihydroxides of aluminum. They are not oxide hydroxides even though, for example, gibbsite is commonly written as $Al_2O_3 \cdot 3H_2O$ for better understandment. Consequently, boehmite and diaspore are also incorreclty referred as “aluminum oxide monohydroxide”, because both a real oxide hydroxides, AlO(OH). Boehmite is also commonly written as $Al_2O_3 \cdot H_2O$.

Molecular water has only been determined in poorly crystallized pseudoboehmite. (Hudson *et al*[1], 2000)

2.2.1 Gibbsite and boehmite

According to Slade *et al*[2] (1991), the basic form of gibbsite consists of double layered OH^- ions where each layer has hexagonally packed oxygen atoms. The aluminum atoms are arranged inside the layers coordinated in octahedral formation in hexagonal rings. The OH groups in adjacent layers are directly opposite of each other (cubic packing). Hydrogen bonds are formed to adjacent double layers between OH groups (Wefers and Misra[3], 1987). Slade *et al*[2] (1991) continue that boehmite on the other hand is formed from units containing octahedral coordinated aluminum atoms which are then linked forming layers. Hydrogen atoms are connected at the top and at the bottom of the layers. The layers are held together by hydrogen bonds between the OH groups (Wefers and Misra[3], 1987) Figure 2 presents the structure of gibbsite and boehmite.

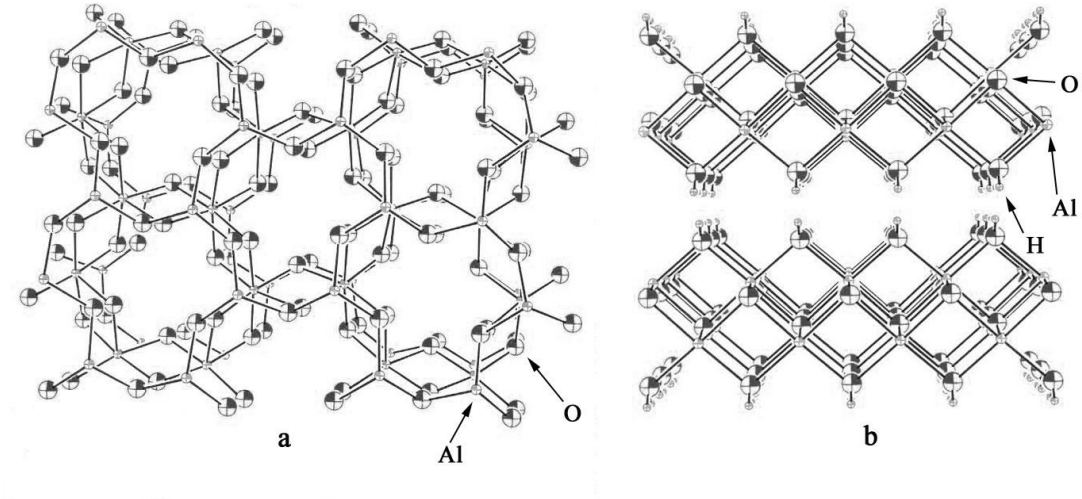

Figure 2. The structure of a) gibbsite (view from top, hydrogen atoms are not shown) and b) boehmite (side view). (Modified from Wefers and Misra[3], 1987)

2.2.2 Alpha alumina and transition aluminas

Alpha alumina (α-Al_2O_3), or corundum, is the only thermodynamically stable oxide of aluminum. Wefers and Misra[3] (1987) reported that the alpha alumina has a trigonal structure where every aluminum atom is coordinated octahedrally to six oxygen atoms. Two thirds of the octahedral interstices are occupied with Al^{3+} ions

to maintain electrical neutrality. However, the structures of transition aluminas are under certain amount of debate. Alpha alumina is presented in figure 3.

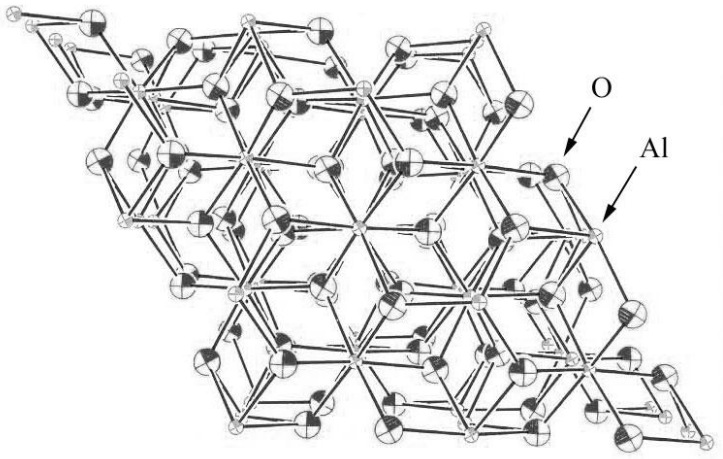

Figure 3. The structure of alpha alumina (α-Al_2O_3). (Modified from Wefers and Misra[3], 1987)

The alumina forms that are produced before alpha alumina are referred as transitional aluminas. The reaction pathway can be seen in section 3.1, figure 4. These aluminas conclude gamma, delta, theta, chi and kappa aluminas. Wefers and Misra[3] (1987) reported that gamma alumina (γ-Al_2O_3) has a spinel, essentially a cubic, structure (two cubic structures inside a bigger lattice). Some authors (Paglia *et al*[4], 2003) have reported a gamma-prime (γ'-Al_2O_3) phase also to occur. It is a phase similarly structured as the gamma phase but with slight uncertainty in the structure. Delta alumina (δ-Al_2O_3) is reported to have a similar formation than the gamma alumina. It has actually been concluded that there is no real difference between gamma and delta alumina forms (Gan[5], 1996). Wefers and Misra[3] (1987) continue that theta alumina (θ-Al_2O_3) is also related to the spinel structure. However, there is no agreement on the structure of chi alumina (χ-Al_2O_3). Several proposes have been given but the key issue is that it is different than the previous types and therefore it has not a spinel structure. Different researchers debate whether it has a cubic or a hexagonal symmetry. Wefers and Misra[3] (1987) have reported that it is anyhow highly disordered. Kappa alumina (κ-Al_2O_3) suffers also from confusion related to the structure. The conversation is whether the symmetry in kappa alumina is hexagonal or orthorhombic.

3 CALCINATION

When the temperature of aluminum hydroxide is raised over 1100 °C alumina and steam are formed. The reaction is endothermic and the current energy consumption for the entire calcination process according to Klett *et al*[6] (2007) is 2850 kJ/kg alumina. This value also includes the evaporation of the surface moisture on the aluminum trihydroxide. The theoretical value to produce smelter grade alumina (low LOI and low α-Al_2O_3 content but high γ-Al_2O_3 content) is roughly 2100 kJ/kg alumina (Ullmann's[7], 1973) . The calcination reaction can be presented as

$$2Al(OH)_3 \rightarrow Al_2O_3 + 3H_2O(g) \quad (1)$$

At the moment the process is done in circulating fluidized bed reactors (CFB, see section 4.4.2). Previously the operation was done in rotary kilns which were as wide as 3,5 m and had a length of over 80 m. The kiln rotates inclined with a small angle where moist $Al(OH)_3$ is fed from the upper end and slowly falls to the lower end. The $Al(OH)_3$ rolls down against a hot stream of gas which is formed by burning natural gas or oil at the discharge end of the rotary kiln. The energy consumption for this process is 5500 kJ/kg alumina. After a heat recovery system was introduced to the rotary kiln process the energy consumption was lowered to 4200 kJ/kg alumina. The adoption of large capacity stationary calciners enabled the reduction of energy consumption. (Hudson *et al*[1], 2000)

According to Hudson *et al*[1] (2000), the alumina that is calcined in stationary calciners has a higher surface area and also lower alpha alumina content than alumina that is calcined in rotary kilns. The characteristics of the metallurgical grade alumina are controlled by the temperature and the residence time of the calcination as shown in further sections. Some requirements for smelter grade alumina are for example that 92 % of the alumina has to have a particle size over 45 µm and LOI (see section 3.2) has to be below 1,0 percent.

3.1 Thermal decomposition of aluminum hydroxide

As aluminum trihydroxides or oxide hydroxides are heated they start to undergo compositional and structural changes. Ultimately, all of the material is converted into alpha alumina. Interestingly, the heat of the overall decomposition sequence

has some exothermic nature since the reaction from gamma alumina to alpha alumina is exothermic (HCS Chemistry[8]). The generally accepted different reaction pathways for the dehydration reactions are shown in figure 4. Hudson *et al*[1] (2000) reported that the internal porosity of the particles rise considerably since the particles lose mass rapidly but the habit of the crystals changes only a little. Due to this, calcined alumina may have a specific surface area (SSA, total surface area per unit of mass) of several hundred square meters per gram. The SSA is one of the alumina quality measures. A large specific surface area is beneficial for the aluminum smelters due to the fact that the adsorptivity of the particle is naturally higher when it has a larger SSA.

Consequently, particles shrink by rupturing due to the loss of water. Zwicker[9] (1985) has reported an average loss of 16 % of the particle size when heating up aluminum trihydroxide up to 900 °C. Zivkovic and Zilipovic[10] (1981) had also determined that the shrinkage of the particle would be between 10 and 18 % during calcination.

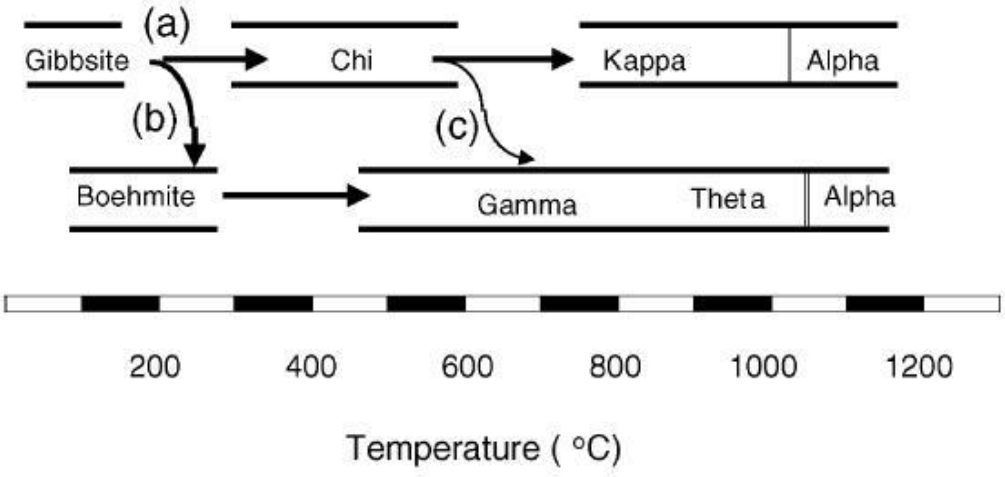

Figure 4. The thermal decomposition of aluminum hydroxide. Pathway (a) is reported to happen with small gibbsite particles (particle size < 50 µm), pathway (b) with large gibbsite particles (particle size > 50 µm) and pathway (c) upon flash calcination of gibbsite. (Modified from Wefers and Misra[3], 1987)

The simplest transformation is the direct change from diaspore directly to corundum (not shown in figure 4). A temperature of roughly 590 °C is sufficient for the complete conversion and the reaction requires only little structural rearrangements. A more complex transformation sequence is the conversion of boehmite and the trihydroxides into α-Al_2O_3. As shown in figure 4 a temperature of 1100 °C is needed until the transformation is complete. Ollivier *et al*[11] (1997) actually claimed that the reaction pathway in industrial calcination processes is mainly via chi alumina and partially via gamma alumina (pathways a and b in figure 4).

Initially, protons diffuse into the adjacent OH groups in the molecule leading to the formation of water. This process begins at temperatures near 200 °C. The water then diffuses out of the particles but if water is trapped inside large trihydroxide particles diffusion becomes a problem. The water cannot diffuse rapidly causing the formation of boehmite. There are few proposals in why the water cannot escape the centre of the particle. Mainly the proposals involve a shell that is on the surface of the particle. For example, Naumann *et al*[12] (1983) suggested that an impermeable chi alumina surface is formed and therefore the water cannot escape causing the formation of boehmite. Another proposal is the presence of a gibbsite shell. The shell hinders the escape of water causing the formation of boehmite. Nevertheless, it is generally accepted that the dehydration reaction of gibbsite via boehmite is more likely to happen with large gibbsite particles (particle size over 50 µm). It has also been suggested that boehmite stops forming due to the fact that the hydrothermal conditions inside the particle will subsequently crack the particle (De Boer *et al*[13], 1953). Consequently, boehmite is not expected to form in smaller particles as water is able to escape easier.

As shown in figure 5 the highest specific surface area of the solid is obtained when the material is calcined around 400 °C. The surface area rises rapidly and lowers almost as rapid after the temperature is further increased. On the other hand, the density of the solid shows progressive growth towards higher temperature values.

However, the reaction sequences such as from gibbsite to corundum or from gibbsite to boehmite and from there to corundum are not the only ones. Ingram-Jones *et al* [14] (1996) have proposed a different path. They proposed that gibbsite decomposes into gamma alumina via chi alumina when the material is subjected to high heating values (pathway c in figure 4). This pathway is therefore reported to happen upon flash calcination of gibbsite where gibbsite is heated extremely rapid (roughly 15 000 °C s^{-1}). Whittington and Ilievski[15] (2003) have also reported such observations with the exception that they broadened the perspective saying that the cross-over can also happen in lower heating rates than what occur upon flash calcination. Yamada *et al*[16] (1984) have also proposed a different route of transition forms. In their proposition, gibbsite decomposes mainly via chi alumina to a pseudo-gamma alumina. From there on the pathway is similar to the one proposed by Ingram-Jones *et al*[14] (1996). Anyhow, Yamada *et al*[16] (1984) have been criticized for the accuracy of their quantification methodology since they did not detail the characterization of their materials.

3.1.1 The effect of the partial pressure of water to the reaction pathway

Naturally, if there is no attempt to remove water from the calciner it will start accumulating. When higher heating rates are used the dehydration rate will also be faster which leads to the fact that the partial water pressure will be higher near the particles. Interestingly, Rouquerol *et al*[17] (1975) have reported that even though boehmite is not supposed to be formed when calcining small gibbsite particles, water pressure near gibbsite particles influences the decomposition pathway. Boehmite was reported to be found when calcining gibbsite particles as small as 1 µm. When the partial pressure increased the amount of boehmite became larger. Sucech and Misra[18] (1986) have also reported a very low loss on ignition value when calcining in hydrothermal conditions (discussed later, see section 3.2.1).

3.1.2 The effect of water after calcination

The surface of the alumina has polar nature and therefore it has a strong affinity for water. In addition, the surface of certain transition aluminas can actually be rehydrated if water is present. For example, rho alumina (ρ-Al_2O_3, and eta alumina, η-Al_2O_3, are also transition aluminas but are not covered in this work) can react with water forming bayerite or gibbsite. Which one of them depends on what

the hydration temperature and water pressure (Wefers and Misra[3], 1987). There are other examples listed by Wefers and Misra but the bottom line is that the analytical work related to the measurement of moisture content might sometimes be difficult in alumina. Hence, alumina should always be kept in a dry place such as an exsiccator and at fairly low temperatures.

3.2 Loss on ignition

Loss on ignition (LOI) states the amount of water that can be removed from aluminum trihydroxide. Consequently, the LOI is a potential weight loss caused by the evaporation of water from calcined material. In the calcination reaction (1) the stoichiometric maximum of steam generated from aluminum trihydroxide is 34,65 percent of the weight of the raw material. Thus, the material consisting a 100 percent of aluminum trihydroxide has a LOI of 34,65 percent and is therefore considered uncalcined. On the other hand when the amount is zero, the material consists entirely of aluminum oxide and is held as fully calcined. LOI is presented as a function of temperature due to the fact that it is predominantly affected by it. Figure 5 shows a typical LOI curve.

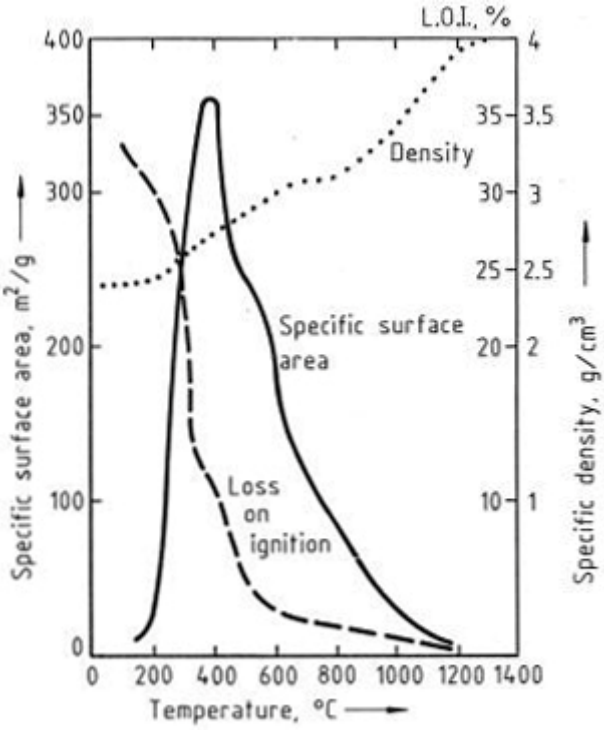

Figure 5. Loss of ignition (LOI), specific surface area and density presented as a function of temperature. (Adapted from Hudson *et al*[1], 2000)

As shown if figure 5, calcination is at its rigorous state below temperatures of roughly 500 C°. This is the most interesting part of this thesis since the LOI can be greatly affected by temperature in this section. As the temperature increases calcination goes on further until LOI reaches a value close to zero. The LOI-value of alumina leaving the calcination process should be lower than one percent and this is why the LOI measurement is a standard in the alumina industry to state one of the product qualities. The analytical way of determining LOI is presented in chapter 6.

Figure 5 shows the LOI curve as it is formed with practical work. On the other hand the curve can be calculated with HSC Chemistry[8], a program to calculate the thermodynamics of a reaction and therefore to estimate the course of the reaction. Figure 6 presents the LOI curve as calculated with HSC Chemistry[8] for the reaction of gibbsite to alpha alumina without the formation of boehmite in between. The reaction is calculated in atmospheric pressure.

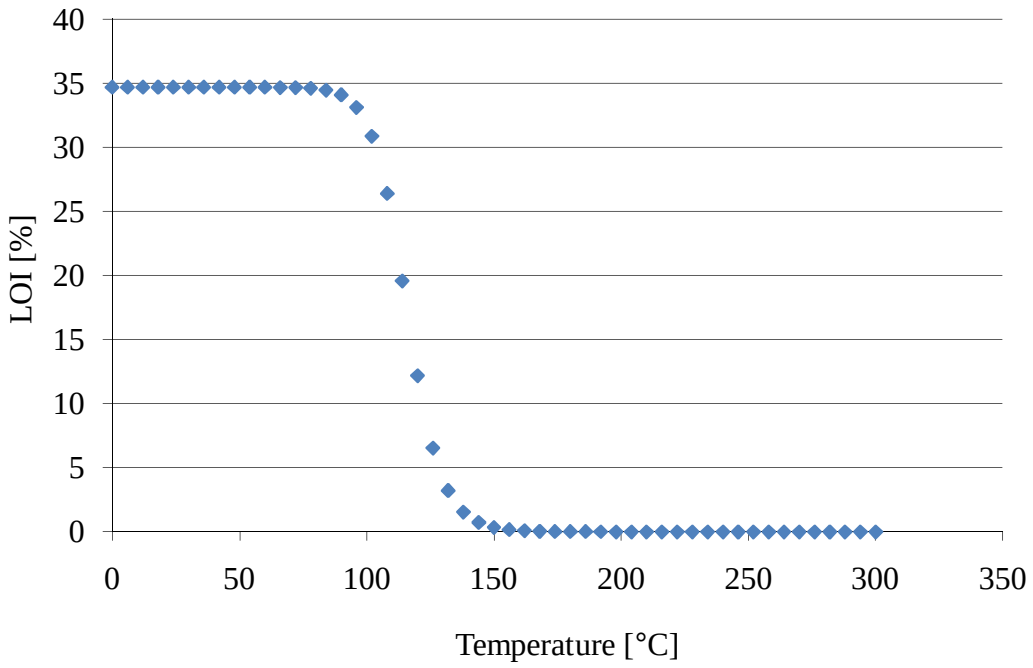

Figure 6. Loss on ignition (LOI) calculated with HSC Chemistry[8] for the reaction of gibbsite to alpha alumina without the formation of boehmite in between (atmospheric pressure).

Figure 6 presents different values that were shown in figure 5. It clearly presents that the LOI-values are close zero and that the material is fully calcined already close to 200 °C. The entire calcination would therefore be completed with less than a half of the temperature usually required in industrial applications. This is due to the fact that HSC Chemistry[8] presents equilibrium results resulting from infinite reaction time. This indicates that the residence time is a serious factor in calcining aluminum trihydroxide into alumina. However, these results are naturally not attainable in industrial processes where residence times are fairly low.

3.2.1 The effect of pressure to loss on ignition

The effect of pressure can a be calculated using HSC Chemistry[8]. Figure 7 presents three LOI curves calculated for the reaction of gibbsite into alpha alumina again without the formation of boehmite in between using 101, 405, 811 and 1378 kPa pressures.

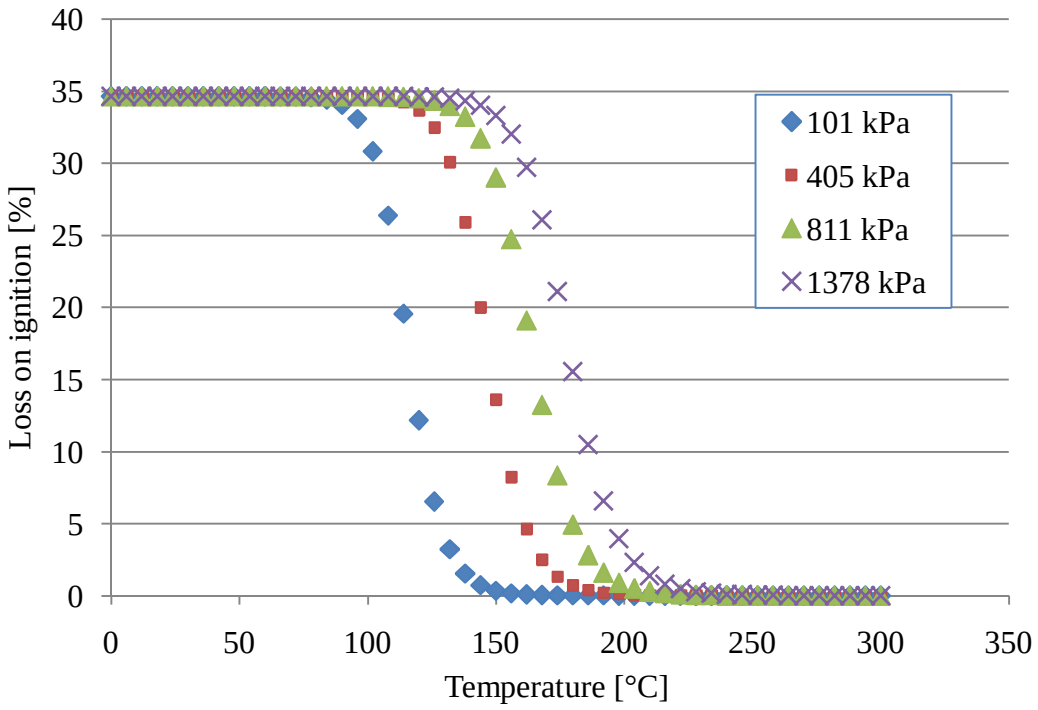

Figure 7. Loss on ignition curves calculated for the reaction of gibbsite to alpha alumina without the formation of boehmite in betweeen in 101, 405, 811 and 1378 kPa pressures.

Again, the material is again fully calcined in lower temperatures than in industrial applications. Clearly HSC Chemistry[8] shows that pressure hinders the calcination.

This can be explained Le Chatélier's rule which states: If a chemical system in equilibrium experiences a change in consentration, temperature, volume or total pressure, then the equilibrium shifts to partially counter-act the imposed change. As the pathway from gibbsite to alumina can be:

$$Al_2O_3 \cdot 3H_2O \rightarrow Al_2O_3 \cdot H_2O + 2H_2O(g) \quad (2)$$

$$Al_2O_3 \cdot H_2O + 2H_2O(g) \rightarrow Al_2O_3 + 3H_2O(g) \quad (3)$$

the equilibrium is shifted towards the direction of the least amount of gas moles when the pressure is increased. In this case, the equilibrium is shifted towards the beginning of the reaction to the side of boehmite. Consequently, this slowes down the calcination and therefore the LOI values with high pressure should be higher than with low pressure.

The effect of pressure to lower the LOI in calcination has been studied by Sucech and Misra[18] (1986). They calcined aluminum trihydroxide in two stages. In the first stage the hydroxide was heated indirectly to the desired temperature in a decomposer vessel. The decomposer vessel was a modified autoclave which was brought to pressure and temperature starting with a small amount of water (hydrothermal calcination). Dry hydroxide was possible to be inserted with pressurized gas. After the first stage the hydroxide was fully calcined in an electrical furnace for one hour in atmospheric pressure. They ran their first stage tests with pressures between 405 and 3040 kPa temperatures between 250 and 650 °C. The results of their test work are presented in figure 8.

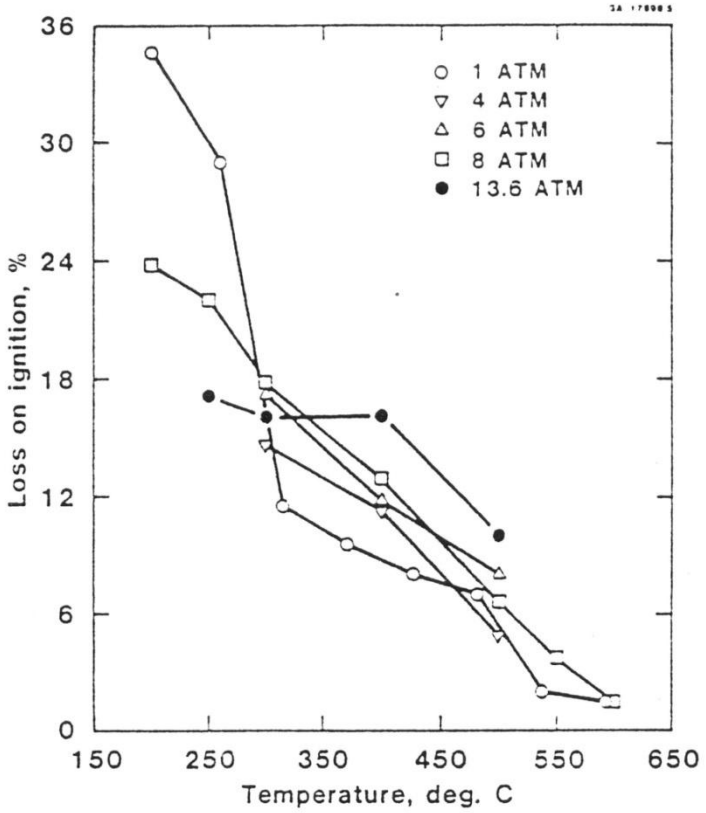

Figure 8. Loss on ignition presented as a fuction of temperature. Five different pressures are used: 101, 405, 608, 811 and 1378 kPa. The temperature range was 250-650 °C. The residence time is unknown. (Adapted from Sucech and Misra[18], 1986)

As shown in figure 8, pressure significantly lowers the LOI especially in the temperature region of 150 and 300 °C. The values for the LOI are roughly 17 and 22 % in athe temperature of 250 °C when using pressures of 811 and 1378 kPa (8 and 13,6 atm). The LOI value is close to 30 % in atmospheric pressure at the same temperature. It seems that they managed to increase the speed of calcination with pressure (assuming that they used the same residence time in all tests). Furthermore, pressure seems to influence LOI also in higher temperatures the exact opposite way it did in lower temperatures. Unfortunately, Sucech and Misra[18] (1986) did not state the residence time for these results. It is stated that all of the test work related to the article were done with residence times between 30 and 120 minutes but the precise time for these results is unavailable.

The fact is that their results are somewhat unordinary. The results they have in the lower end of the temperature range are inconsistent with the theoretical point of

view. As HSC Chemistry[8] presents in its equilibrium calculations, pressure does not lower LOI but on the other hand it hinders calcination and therefore makes LOI higher in a given temperature. The results presented by Sucech and Misra[18] (1986) are the exact opposite as calculated thermodynamically. However, their results seem to be correct after the lines have crossed 350 °C. At this section and beyond the highest curve (highest LOI) is the one with the highest pressure followed by the second highest pressure ending up to the curve with 101 kPa pressure. These results are then same as the ones calculated by HSC Chemistry[8].

A simple kinetical investigation is also contrary to the results Sucech and Misra[18] (1986) have proposed. For example, if the kinetics of the rate of calcination would be expressed as:

$$v_{calcination} \propto k(P_{H_2O}^{eq} - P_{H_2O}^{prevalent}) \quad (4)$$

where
- k — reaction rate coefficient, [-]
- P^{eq} — equilibrium pressure, [kPa]
- $P^{prev.}$ — prevalent steam partial pressure, [kPa]

the driving force of the reaction is the pressure difference between the prevalent partial pressure of steam and the equilibrium pressure. The equilibrium pressures of the reactions from gibbsite to alpha alumina are expressed in the following table:

Table I. Equilibrium steam pressures for reaction (2) and (3) in various temperatures. (HSC Chemistry[8])

Temperature [°C]	Reaction (2) [kPa]	Reaction (3) [kPa]
100	51,6	0,3
150	533,4	6,2
200	3313,1	76,7
250	14272,1	607,6
275	26621,0	1501,8

As shown, the equilibrium pressures are extremely high at temperatures over 250 °C. Therefore, even if the partial pressure of the steam would be very high it still

not would be high enough to stop calcination. The reaction can only be influenced with pressures such as 1378 kPa (13,6 atm) at temperatures under 150 °C for reaction (2) and 275 °C for reaction (3). In addition, the kinetics state that if the partial pressure of the steam is increased this will slow down the rate of calcination and definitely not speed it up regardless of th reaction rate coefficient, k, values as well if the equation has a power (the values of k and possible powers are insignificant in this matter). Therefore, it is quite strange that Sucech and Misra[18] (1986) had a lower LOI in higher pressures assuming that they used the same residence time for all tests. Due to this, their results have to be considered with serious doubt.

To conclude, pressure should not influece the LOI in a lowering way but on the other hand increase it. Le Chatélier and kinetics state that the reaction should move towards the raw materials and not the product and that the rate of calcination could only be slown down and not increased.

4 FLUIDIZED BED REACTOR

A fluidized bed reactor can be operated as a batch or as a continuous reactor. The bed is usually operated in the aggregative regime (see section 3.1.1) to provide total fluidization of the solids. However, the gas velocity has to be low enough to prevent solids from being carried out of the vessel. The essential elements of a fluidized bed reactor are presented in figure 9.

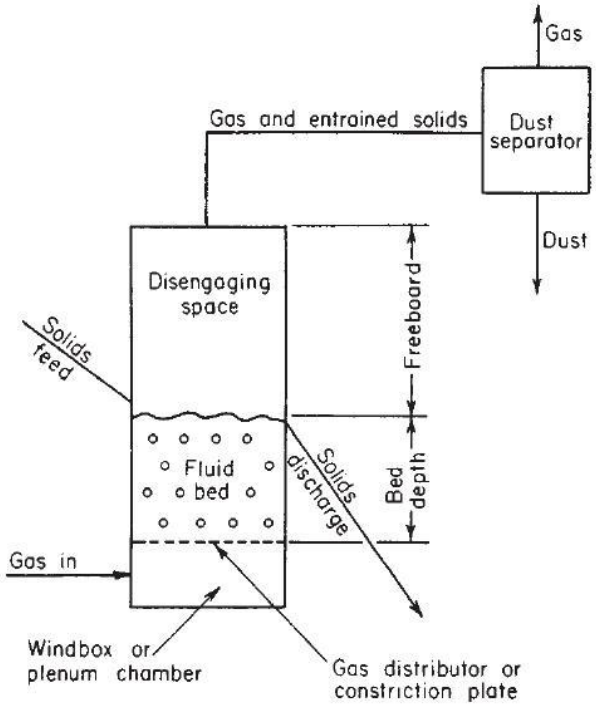

Figure 9. The essential elements of a fluidized bed reactor. (Adapted from Perry's[19], 1997)

As shown in figure 9, the essential elements of a fluidized bed reactor are the vessel itself, the bed and the disengaging space portion, gas distributor, solids feeder and solids discharge, the dust separator for the exit gases and the gas supply. The most common geometrical shape for the vessel itself is a cylindrical form. The height of the cylinder is determined by the depth of the bed and the vertical expansion of the solids. The disengaged splashed and elutriated solids must also be taken into account. Basically, the same properties are used when designing a vessel for boiling liquid. The width of the vessel is determined by the desired volumetric gas flow or on the other hand, the velocity of the gas required. Different conditions might be wanted but carry-over of the particles is not accepted. Therefore, the maximum flow is generally determined by the carry-over of the particles. The bed height is determined by the gas' contact time with the solids as well as the residence time of the solids in the bed. Usually the bed is not lower than 0,3 m but on the other hand not higher than 15 m. As shown, the volume between the bed surface and the exit gas outlet is called the disengaging space (freeboard). Mainly two different phenomena can happen in this section: a reaction between the gas and the particle or the classification of the particles where lighter and finer

particles are carried upwards while coarse particles drop down to the surface of the bed. (Perry's[19], 1997 and Geldart[20], 1986)

The gas distributor has a considerable effect to the fluidization properties. Basically, there are two types of gas distributors: a type where solids are carried with the fluidizing gas (for example grids of T bars or concave perforated plates) and a type where the fluidizing gas is clean (more sophisticated designs such as the Insert Tuyere and Clubhead Tuyere, see Perry's[19], 1997, for more information). The latter distributor is designed in a way that the back flow of the particles is possible neither in operation nor in the shutdown of the reactor. Naturally, the material of the gas distributor as well as the entire system must be able to stand the very high temperatures (see chapter 2, Calcination). The dust separator usually located external from the reactor is used to separate the fine and light solids carried out of the vessel. The solids may be re-circulated or removed as dust. The gas however passes the system only once. (Perry's[19], 1997)

4.1 Fluidization

Fine solids are transformed into a fluid like state through contact with liquid or gas. This is called fluidization. The fluid flows from the bottom of the vessel lifting the particles up into a state where the solids look and behave as boiling liquid. According to Kunii and Levenspiel[21] (1991), a large object will pop up onto the surface of the bed and float (the density of the object must be lighter than the bulk density of the bed) when it is pushed into the bed and released. Furthermore, the surface of the bed will remain horizontal when the entire column is tipped. If two beds with different amounts of solids are connected their surfaces will equalize as would also happen with liquid. Moreover, the bed has also flow properties of a liquid. If one was to make a hole onto the side of a column the solids would burst out as a jet. The solids can also be made to flow liquid-like from a vessel to another vessel.

4.1.1 Fluidization regimes

Fluidization regimes can be categorized into five different categories. All of the regimes where fluid passes through a bed are fixed bed, particulate regime, aggregative fluidization, fast fluidization and pneumatic conveying. Quite obviously,

the first and last are not held as fluidization since in the first regime fluidization does not yet take place and the last one is related to the transportation of solids and not to fluidized beds. Figure 10 shows the all of the different regimes. (Kunii and Levenspiel[21],1991 and Perry's[19], 1997)

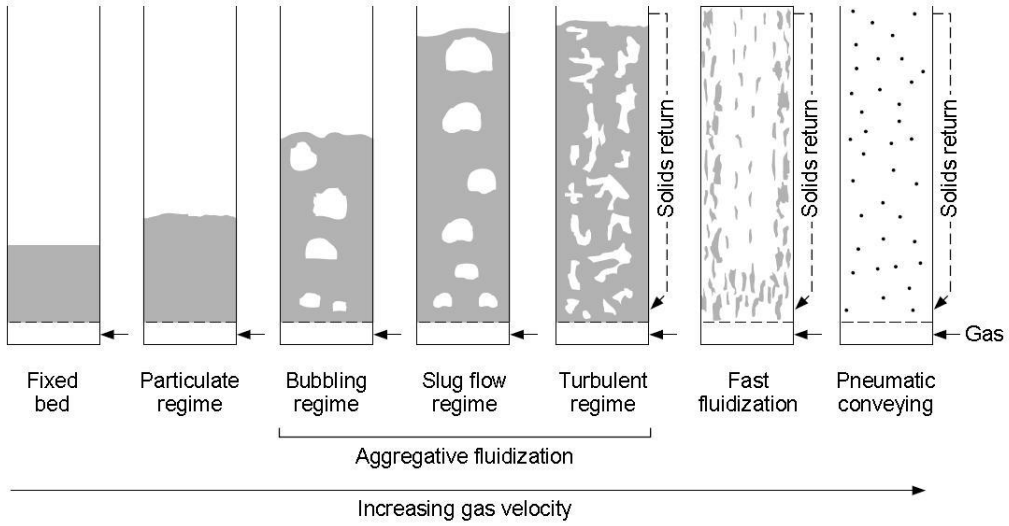

Figure 10. Different regimes of fluidization. Gas velocity increases to the right. Fluidization does not take place in the fixed bed. Solids are transported in pneumatic conveying. (Adapted from Perry's[19], 1997)

Fluidization begins when fluid is fed through a bed of particles. The first regime is the fixed bed regime where the fluid is blown through the particles without moving them. The particles therefore keep stationary. The gas flow merely passes the particles through the voids between them. This leads to the fact that the particles are very loose at this moment. The pressure drop across the bed is also linear (see section 3.2, minimum fluidization velocity). When the velocity of the fluid becomes larger the particles start to move. The particles start to vibrate and the bed is slightly lifted from its fixed bed state. The fluid which flows through the bed still does not have enough energy to entirely lift the particles up even though the bed is in an expanded state. When the velocity is further increased, the fluid no longer filters through the solid particles but starts to push them upward. The gravitational pull on the particles is still too strong but when velocity increases the drag force of the fluid matches the gravitational pull of the particles. This is called the fluidization state (see section 3.2, minimum fluidization velocity). The bed starts

to fluidize without the formation of bubbles (particulate regime). (Kunii and Levenspiel[21], 1991)

When the flow rate of the gas is further increase the bed regime changes into the aggregative regime. First, bubbles start to form on to the surface of the bed (see minimum bubbling velocity, section 3.3). The mixing of solids is rigorous at this point. Fluidized beds are considered to be stable when operated in the expanded state but change into an unstable state when bubbles start to form. The bed does not expand much after the minimum fluidization velocity has been reached. Channels might be formed instead of bubbles which will decrease the amount of fluidization. Slugging may appear when the gas velocity is increased from the minimum bubbling velocity. Slugs are large bubbles due to coalescence in the bed and are greatly affected by the geometry of the column. It is problematic since it hinders the performance of the bed and increases the problems of entrainment. This is due to the fact that slugs may be as wide as the entire vessel. This leads to the lifting of a portion of the bed which is especially problematic in long and narrow beds. (Kunii and Levenspiel[21], 1991)

Finally, the velocity of the fluid is high enough the slugging disappears and the bed enters turbulent conditions. The velocity of the fluid has now exceeded the gravitational pull on some of the particles and lead to the carryover of the smaller particles out of the vessel. The particles must then be re-circulated back into the bed. Right after the turbulent conditions when the velocity of the fluid is high enough to exceed the terminal velocity (a falling particle will accelerate due to gravitational force until the drag of the fluid balances it) of all the particles in the bed, fast fluidization conditions have been reached. All of the particles are carried out of the vessel and must be re-circulated. A dense phase in the bed cannot be clearly defined anymore since there is no clear upper limit or surface to the bed. The last state is therefore the total transportation of the solids in a vessel. Here, the fluid velocity has greatly exceeded the terminal velocity and therefore particles are vastly carried out of the vessel. (Kunii and Levenspiel[21], 1991)

4.2 Minimum fluidizing velocity

When the gas that is fed vertically through a packed bed has a velocity high enough to start fluidizing the particles it has reached the minimum fluidization

velocity, U_{mf}. Before the bed is fluidized the pressure drop of the gas over the bed increases as the velocity of the gas increases. The bed is then lifted gently. This happens until the drag on an individual particle becomes stronger than the gravitational pull or the pressure drop across the bed equals the weight of the bed per unit area. The particle size affects the minimum fluidization velocity greatly. As the particle size increases the kinetic energy must increase in order to keep the fluidization running. Otherwise the bed collapses and fluidization stops. When U_{mf} is reached the pressure drop becomes constant as the bed is fully supported by the flow of the gas. Figure 11 shows the pressure drop as a function of the fluidization velocity. (Geldart[20], 1986)

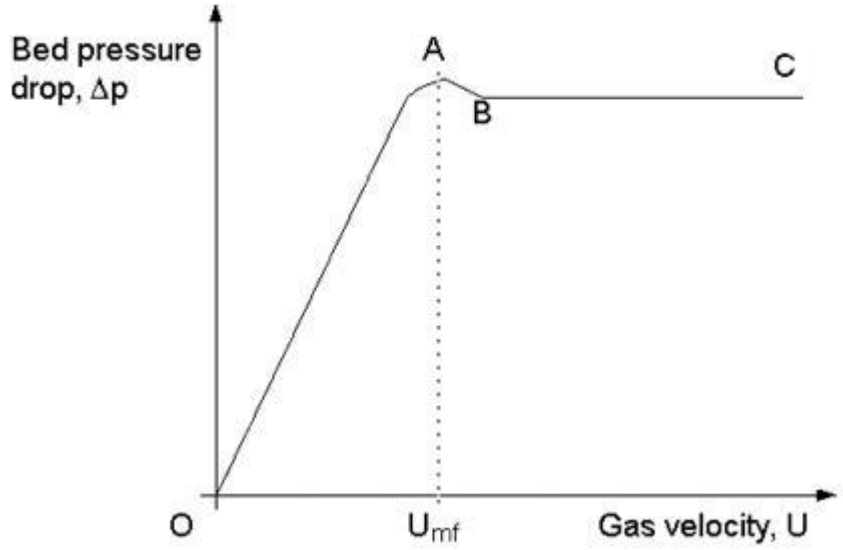

Figure 11. The bed pressure drop as a function of the gas velocity. The pressure drop is linear between O and A ("packed bed" region). Minimum fluidization occurs at point A and between B and C the bed is completely fluidized. (Adapted from Particle Technology Phenomena[22])

The pressure drop (ΔP) can be calculated with the Ergun[23] (1954) equation. It can be used for non spherical particles over a wide range of Reynold's numbers. Ergun showed in his equation that the total pressure drop in a fixed bed is dependent on the flow rate of the fluidizing medium, bed voidage (ε), particle shape (φ_s) and size (d_p). Furthermore, it is shown that the pressure drop across a fixed bed is the sum of viscous and kinetic energy losses. The Ergun equation is stated as:

$$\frac{\Delta P}{L} = \frac{150(1-\varepsilon)^2}{\varphi_s^2 \varepsilon^3} \frac{\mu U_{mf}}{\left(d_p^2\right)} + \frac{1{,}75(1-\varepsilon) U_{mf}^2 \rho_f}{\varepsilon^3 \varphi_s d_p} \tag{5}$$

where

L		length of the bed, [m]
d_p		particle size, [m]
ρ_f		fluid density, [kg m^{-3}]
μ		fluid viscosity, [Ns m^{-2}]

As mentioned, at U_{mf} the pressure drop is equal to the bed weight per unit area. This is presented in the following equation:

$$\frac{\Delta P}{L} = (1-\varepsilon)(\rho_p - \rho_f) g \tag{6}$$

where

ρ_p		particle density, [kg/m^3]
g		acceleration due to gravity: 9,81 [m/s^2]

Furthermore, equations (5) and (6) can be combined to give a dimensionless form of the Ergun equation as follows:

$$Ar = 150 \frac{(1-\varepsilon)}{\varphi_s^2 \varepsilon^3} \mathrm{Re}_{mf} + \frac{1{,}75}{\varphi_s \varepsilon^3} \mathrm{Re}_{mf}^2 \tag{7}$$

where Ar is the Archimedes number and Re_{mf} the Reynold's number at minimum fluidization velocity. They are expressed as:

$$Ar = \frac{d_p^3 \rho_f (\rho_p - \rho_f) g}{\mu^2} \quad \text{and} \quad \mathrm{Re}_{mf} = \frac{d_p \rho_f U_{mf}}{\mu} \tag{8}$$

Wen and Yu[24] (1966) calculated that the bed porosity as well as the shape factor terms in equation (7) can be approximated as:

$$\frac{(1-\varepsilon)}{\varphi_s^2 \varepsilon^3} \approx 11 \quad \text{and} \quad \frac{1}{\varphi_s \varepsilon^3} \approx 14 \tag{9}$$

These approximations lead to the simplification of equation (7) which can now be written as:

$$Ar = 1650 \,\mathrm{Re}_{mf} + 24{,}5 \,\mathrm{Re}_{mf}^2 \tag{10}$$

Finally, equation (10) can be simplified into a form where the minimum fluidization velocity can be calculated:

$$U_{mf} = \frac{\mu}{\rho_f d_p}\left\{(1135{,}7 + 0{,}0408Ar)^{\frac{1}{2}} - 33{,}7\right\} \qquad (11)$$

The correlation provided by Wen and Yu gives most reliable results when used with particles that have a particle size over 100 µm. Furthermore, there are many other correlations provided for the determination of the minimum fluidization velocity than the one given by Wen and Yu. For example, Delebarre[25] has revisited the equation in 2004. The minimum fluidization velocity can also be determined experimentally. The determination of U_{mf} via a cold fluidization test is explained in chapter 6.

4.2.1 The effect of pressure and temperature to U_{mf}

As it is known, increasing pressure increases the density of a gas. The effect of pressure to the minimum fluidization velocity has been studied by Rowe[26] (1984). For particles with a diameter of about 100 µm the pressure had little or no effect on U_{mf}. As particle size increased to about 500 µm the U_{mf} decreased sharply to a pressure of 20 bar and gradually after that. The pressures used in the experimental part of this work have only values of 0 to 6 bar over pressure. Therefore, the influence of pressure in the fluidization velocity can be held as minimal.

King and Harrison[27] (1982) imply that in fine powders U_{mf} decreases with increasing temperatures. On the other hand, U_{mf} increases in coarse powders. With small Reynolds numbers the viscous term of the Ergun equation is dominant. Because viscosity increases with increasing temperature for a gas, U_{mf} decreases with temperature. For large Reynolds numbers the kinetic term of the Ergun equation is dominant. The density of a gas decreases with an increase in temperature. This means that U_{mf} increases with temperature.

4.3 Minimum bubbling velocity

Minimum bubbling velocity, U_{mb}, can be noticed when bubbles start to form on the surface of the bed. Bubbles appear and disappear when the side of the column is gently tapped. The formation of bubbles is very dependent on the type of powd-

er (Geldart's classification of powders to groups A-D, not covered in this work). For example, group C powders which are very cohesive, cannot form bubbles. The powders are fluidized with velocities higher than the minimum fluidizing velocity. On the other hand, bubbles form already at the minimum fluidizing velocity for group B powders which are typically sands (particle size between 60 and 500 µm). When the fluid velocity is further increased bubbles start to periodically burst from the surface of the bed. This causes the bed to collapse rapidly. If the gas velocity is then decreased bubbles disappear and the bed is once again quiescent. For deep beds the maximum bed height is usually achieved at the minimum bubbling velocity. (Geldart[20], 1986)

According to Yates[28] (1996), most of the work devoted to the effects of temperature and pressure in bubbling fluidization is widely related to the hydrodynamics and voidages of the bubbling beds. However, bed stability should increase with increasing the pressure. Bubble size is differs with pressure but is also dependent on Geldart's groups A, B and D. The effects of temperature in the bubble dynamics are a relatively unknown area and furthermore, the results available are contradictory.

4.4 Industrial applications of fluidized bed reactors

Fluidized beds are widely used in industry and are generally used in the contacting of gas and solids. The fluidization technique was first used as early as 1926 for the gasification of powdered coal. It was in the 1940's when its broad use began. In 1940 the first fluidized bed catalytic cracker (FCC) was built . Fluidized bed operations can be divided into physical operations and their use as chemical reactors. The chemical processes are then divided into catalytic and non-catalytic operations as well as the gas-solid reactions. (Kunii and Levenspiel[21], 1991 and Perry's[19], 1997)

Physical operations of fluidized beds are generally applications where relatively large quantities of solids must be treated. These operations may be for example transportation and heat exchange and therefore fluidized beds provide an efficient and convenient method for this operation. Transportation of solids can be done via pneumatic conveying of the particles as discussed earlier in section 3.1.1. However, other types of conveyors are also available. Because of the liquid-like behavior

of the fluidized solids they can be transported via air slide conveyors where solids are fluidized on a plate which is slightly inclined. The solids then move downwards by the force of gravity. (Kunii and Levenspiel[21], 1991 and Perry's[19], 1997)

Fluidized beds are extensively used for heat exchange. The cooling of particles is advantageous in a fluidized bed because the bed has an ability to transport heat rapidly. In calcination, hot alumina particles are cooled down in a fluidized bed where water is used as the cooling medium. The particles enter the bed and move against tubes containing the cooling water. The fluidization gas may be conditioned to prevent it from picking up volatiles such as moisture. The dry solids then move towards the end of the bed where they are discharged. The cool fluidizing gas is separated in a cyclone in the discharge area. (Kunii and Levenspiel[21], 1991 and Niro Inc.[29])

Fluidized beds can be used for other physical operation other than transportation and heat exchange. The mixing of fine powders, coating of plastic materials and metal surfaces as well as drying and classification of powdery materials, adsorption and granulation are important industrial processes not covered by this work. More information is provided by Perry's[19] (1997), Kunii and Levenspiel[21] (1991) and Geldart[20] (1986).

As mentioned, the chemical processes involving fluidized beds are classified into catalytic and non-catalytic processes. Reactions between gas and solids are dealt separately. Geldart[20] (1986) as well as Kunii and Levenspiel[21] (1991) have listed some of the applications where fluidized beds are used as chemical reactors. The catalytic gas phase reactions are hydrocarbon cracking, catalytic reforming, phtalic anhydride manufacture, aniline production, the synthesis of high-density and low density polyethylene, Fischer-Tropsch synthesis, chlorination or bromination of hydrocarbons and the methanol to gas process. Non-catalytic gas phase reactions are listed as the hydrogenation of ethylene and thermal cracking (for example the production of ethylene). Also the use of fluidized beds in biofluidization is increasingly used in food and pharmaceuticals production.

However, the gas-solid reactions are more of interest to this work. Some of these operations are listed as the roasting of sulphide and sulphate ores, calcination of

limestone, aluminum hydroxides and phosphates, combustion of coal and coke, pyrolysis of coal and hydrogen reduction of ilmenite. The next section is devoted to explain how the calcination of aluminum trihydroxide process works in industrial scale.

4.4.1 The Outotec calcination process

The Outotec calcination process (Process description[30]) consists of two separate preheating stages, a calcining stage and two cooling stages. The entire residence time from when the raw material is fed into the process to the point when the product is discharged from the end is roughly twenty minutes. The flowsheet of the process is presented in figure 12.

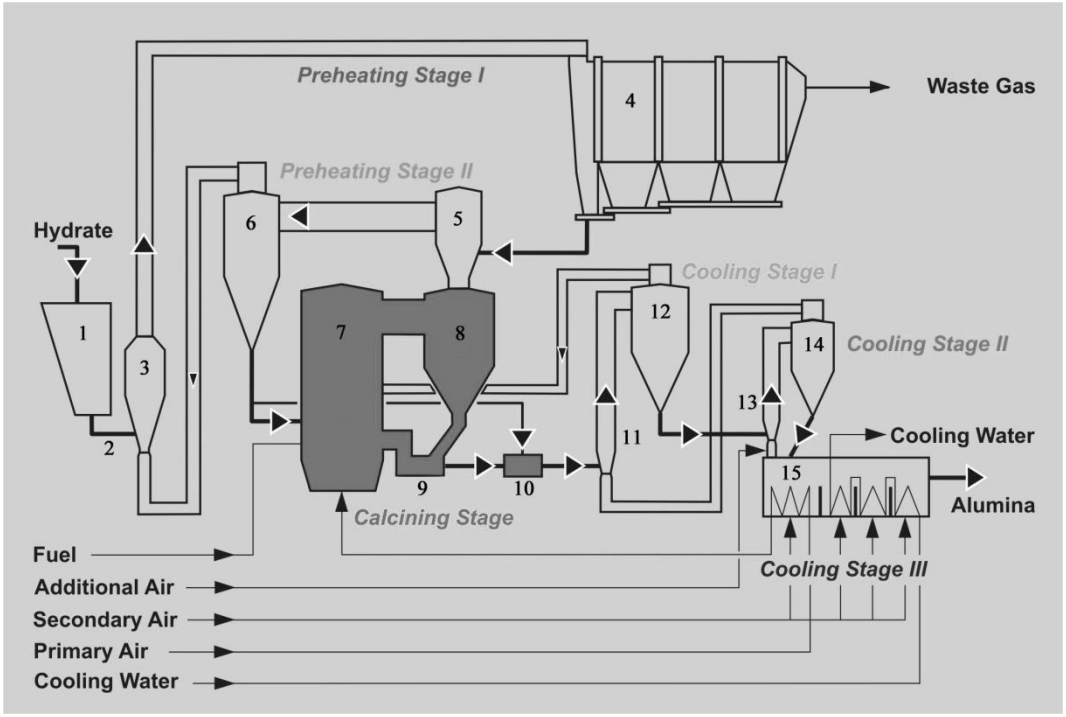

Figure 12. Flowsheet of the Outotec calcination process. The equipment are numbered as 1-15. (Modified from the Process description[30])

Hydroxide is fed into the feed bin (1) from where it is discharged by a dosing belt scale to a screw feeder (2). The screw feeder delivers the material to a venturi preheater (3) which is a part of the first preheating stage. There, the solids are mixed with the waste gas coming from the cyclone (6) of the second preheating stage. The waste gas has enough heat to evaporate the all of the surface moisture on the hydroxide. The preheated hydroxide is carried by the waste gas as into a

two-stage electrostatic precipitator (4). The first stage is a mechanical stage where parts of the entrained solids are precipitated and the rest of the solids together with the waste gas move to the second stage. Here, the waste gas is cleaned by electrostatic precipitation.

The collected solids then move to the bottom of the mechanical stage from where all of the solids move to an air slide which discharges the solids into a sending pot of a pneumatic elevator. From here, the hydroxide is conveyed by air to an airlift cyclone. The solids are discharged via a discharge seal into the lower part of the venturi preheater (5) located in the second preheating stage of the process. The conveying air is taken via ducts to the second air cyclone in the second preheating stage. The air finally serves as combustion air inside the furnace after it has been cleaned in the airlift cyclone.

The hydroxide that has entered the venturi preheater (5) in the second preheating stage is mixed with hot waste gas coming out of the recycling cyclone (8). The hydroxide is partially dehydrated due to the heat in the waste gas. The flow of gas and the solids are then separated in the second cyclone (6) in the second preheating stage. From the second cyclone the main portion of the precalcined material is fed into the fluidized bed furnace. A seal pot acts as a pressure seal in the material feeding into the furnace. A portion of the hydroxide coming from the first preheating stage is bypassed into a mixing pot (10). The amount is adjusted by the loss on ignition value of the alumina product coming out of the cooling section.

The actual calcination of the preheated and partially dehydrated takes place in a circulating fluidized bed furnace (7). Both natural gas and heavy fuel oil can be used as fuel to heat fluidizing air. Because of the velocity of the fluidizing air, solids are carried out of the furnace into the recycling cyclone (8) where air is separated from the solids. The solids return through the furnace seal pot (9) into the furnace. The temperature of both the gas and the solids are nearly identical in all three parts of the calcination stage. The solids are also fluidized inside the furnace seal pot. This is required for the re-circulation of the solids and is done with a seal pot blower.

A solid stream is taken out of the furnace seal pot (9) and fed into the mixing pot (10) that contains material from the first preheating stage. Because the calcined alumina still has a lot of heat the material fed into the mixing pot earlier is also calcined to an appropriate level. Due to the fact that the reaction is principally endothermic the product stream from the mixing pot is cooler than the temperature inside the furnace.

The alumina discharged from the calcination stage is cooled in two direct cooling stages. Both stages consist of a lift duct and a secondary air cyclone. The third cooling stage is designed as a fluidized bed cooler. The alumina coming from the calcining stage is first mixed in a lift duct (11) with preheated air coming from the second cooling stage and conveyed into a secondary air cyclone (12). The air is separated and fed into the furnace as secondary air and used for combustion. The alumina is then fed from the bottom of the cyclone (12) into another lift duct (13) via a pressure seal. The solids are mixed with air coming out from the fluidized bed cooler (15). Once again the particles are conveyed into a cyclone (14). Additional air is provided with blowers. The solids are then discharged into the fluidized bed cooler (15). The cooler works counter currently with air as the cooling medium. Finally water is used for the cooling of the product in the end of the fluidized bed cooler. The final product is discharged from the cooler with a pneumatical transport system.

4.4.2 Elements of a CFB reactor

A circulating fluidized bed reactor consists of a tall main reactor also referred as the “riser” where particles are entrained in a fluid flow. The particles are then carried out of the reactor from the top and separated in a separation device usually located external to the reactor. The particles are then returned to the reactor from the loop seal located below the separation device. Particles may keep circulating this loop many times before they are discharged from the CFB. The fluid however passes the system only once. A typical CFB is shown in figure 13.

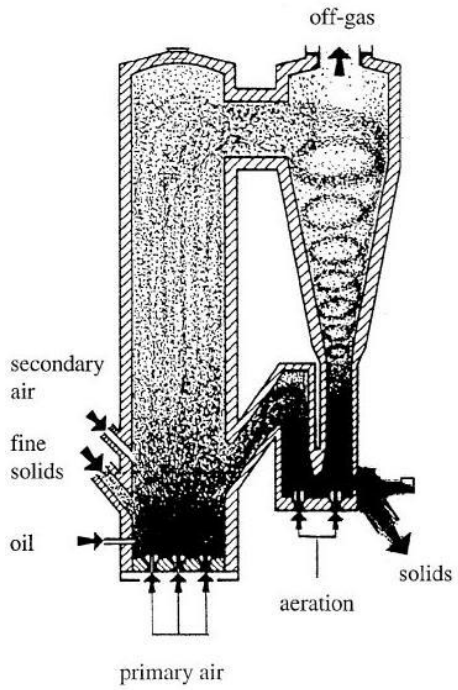

Figure 13. A typical CFB reactor. Solids are fed into the reactor from the left side. Fast fluidization conditions ensure that the solids circulate in the system. Gas is separated from the circulating solids in the external cyclone. The product is discharged from the loops seal located below the separation cyclone. (Adapted from Reh[31], 1999)

According to Yang[32] (2003) the CFB is operated with high fluid velocities that are between 2-12 m/s. The particle flux is also high (typically 10-1000 kg $m^{-2}s^{-1}$) which means that inside the riser there is no distinct interface between the dense phase of the bed and the region above. The contacting with the fluidizing fluid and the solids is therefore done not in the bubbling, slugging or turbulent regimes but in the higher velocity regimes such as fast fluidization. Table II presents the usual operating variables used in commercial operations.

Table II Operating variables of commercial CFB reactors. (Yang[32], 2003)

Superficial gas velocity	2-12 m/s
Net solids flux through riser	10-1000 kg/m^2s
Temperature	20-950 °C
Pressure	100-2000 kPa
Mean particle diameter	50-500 µm
Overall riser height	15-40 m

4.4.3 Advantages and disadvantages of fluidized bed reactors

Fluidized beds used in industrial applications have many advantages. Such advantages are for example the liquid-like flow of the particles or good heat transfer. The downside is that fluidized beds also have disadvantages that either make fluidization problematic or on the other hand hinders the reaction to a non-acceptable level. This section is therefore devoted to discuss the up and downsides of fluidized beds.

Yang[33] (2003), Kunii and Levenspiel[21] (1991) and Geldart[20] (1986) explain that the liquid behavior of the fluidized particles is certainly advantageous, because it enables easy handling of the particles inside vessels and pipelines. Solids can easily be fed and discharged from continuously operating reactors. Furthermore, automatically controlled operations are enabled. Near isothermal conditions inside reactors are quite easily achieved due to the fast mixing properties of the solids. The thermal uniformity ensures that "hot spots" are avoided. Because of this, the operations can be easily and reliably controlled. In addition, as a result of the fast and good mixing of the solids, the whole vessel is thermally resistant to rapid temperature changes. Moreover, the vessel responds slowly to sudden changes in operation conditions and therefore gives a large safety margin to avoid runaways in exothermic reactions. Fluidization of solids gives excellent heat and mass transfer rates between the gas and the solids. Due to the good heat transfer between particles and immersed surfaces, the surface area required for heat exchangers within the vessel is relatively low. Last but definitely not least, fluidized beds are suitable for large scale operations making it possible for their use in industrial applications.

Unfortunately, fluidized beds represent also disadvantages and not only advantages and because of this, considering the limitations of fluidized beds is very important when selecting the type of reactor for a given process. Yang[33] (2003), Kunii and Levenspiel[21] (1991) and Geldart[20] (1986) continue that in bubbling beds the bubble sizes may vary substantially. This might lead to the formation of too large bubbles which then hinder the contacting between the gas and the solids leading to decreasing selectivity. This problem might be overcome by selecting other types of reactors. The rapid mixing of the solids might lead to a non-uniform resi-

dence time of the solids. In CFB's some solids may circulate much longer than others decreasing the uniformity of the final product. Friable solids can be pulverized inside the vessel and then be carries out as dust with exit gas. Also, hard particles can damage the pipelines and vessel by abrasion. Fine solids may begin to sinter and agglomerate when operated in high temperatures. This situation forces the temperature to be lowered and therefore reduces the reaction rate. The particle size limits the possibility to use fluidized bed processes. Generally speaking, if the particle size is smaller than 30 µm fluidization becomes difficult and on the other hand if it is larger than 3,0 mm the same situation occurs. When using fine particles, their entrainment can issue some problems. Expensive or toxic particles carried out of the can cause the need for pollution control equipment which might bring up economic problems. A serious problem is the scale-up of fluidized bed reactors because industrial size reactors have quite often individual fluidization characteristics. Therefore, it is quite hard to predict and model their behavior in operation leading to the fact that each reactor might require special attention.

If CFB reactors are compared to stationary fluidized beds (bubbling fluidized beds) they present better gas to solids mixing and better gas to gas mixing. The particle size range is wider in CFB reactors because of circulation. This is the same reason why the gas velocity used in CFB reactors is easier to determine than in stationary beds. In CFB reactors, the gas velocity must be between a lower and a higher value. It is not very important what the velocity is as long as there are fast fluidization conditions. Stationary beds on the other hand must be fluidized with restricted gas velocities to ensure that entrainment does not occur. Obviously, the residence time in CFB reactors is also different than in stationary beds since stationary fluidized beds can operate with a certain load of solids. CFB reactors can operate with different amounts as long as the velocity of the fluidizing medium is high enough. (Lurgi sheet[34])

5 EXPERIMENTAL EQUIPMENT

The experimental equipment used in this thesis comprised a laboratory scale fluidized bed reactor, a laboratory scale cold fluidization apparatus, two muffle furnaces, a laser diffraction machine, a jet sieve, a differential thermal analysis (DTA) and an X-ray diffractometry apparatus. The actual tests were carried out in

the fluidized bed reactor. The rest of the equipments were for analytical work and particle characterization. All equipments are dealt in detail in this chapter.

The raw material used in all of the tests was dry aluminum trihydroxide delivered from Alunorte Barcarena, Brazil. It had a mean particle size of 132 µm (measured with laser diffraction) and a particle density of 3390 kg/m^3 (measured with a pycnometer by Melnikowitsch[35], 2008).

5.1 The fluidized bed reactor

The laboratory scale fluidized bed reactor used for the calcinations in this work was a steel tube that had a conical top. The reactor had a porous plate in the bottom to enable fluidization. A lid was placed on top of the reactor and locked in place with bolts. The lid itself had a pressure gauge (bar scale) for measuring the inside pressure of the reactor (showing zero bar in atmospheric pressure), a pressure relief valve, a valve to close the material feeding pipe and finally a hole where a thermocouple connected to a temperature meter measuring the inside temperature of the reactor was placed. The thermocouple went through the reactor lid almost to the bottom of the reactor.

A straight steel pipe ran from the bottom of the reactor and was connected to a hose carrying pressurized air. The air itself came from the instrumental air pipeline which could be turned off by a valve. A rotameter calibrated for oxygen in 40 °C and 210,3 kPa pressure measured the airflow. After the rotameter a pressure gauge monitored the pressure of the air flow. Finally a valve controlled the airflow from the rotameter to the steel pipe coming from the bottom of the reactor.

The steel reactor was heated up, by placing it into an electrical heated tube furnace. The tube furnace was equipped with a temperature controller and the corresponding thermocouple. This thermocouple was placed between the pressure reactor and the ceramic inliner of the tube furnace according to Figure 14. With the use of this thermocouple and the second one inside the pressure reactor it was possible to adjust the temperature of the test apparatus.

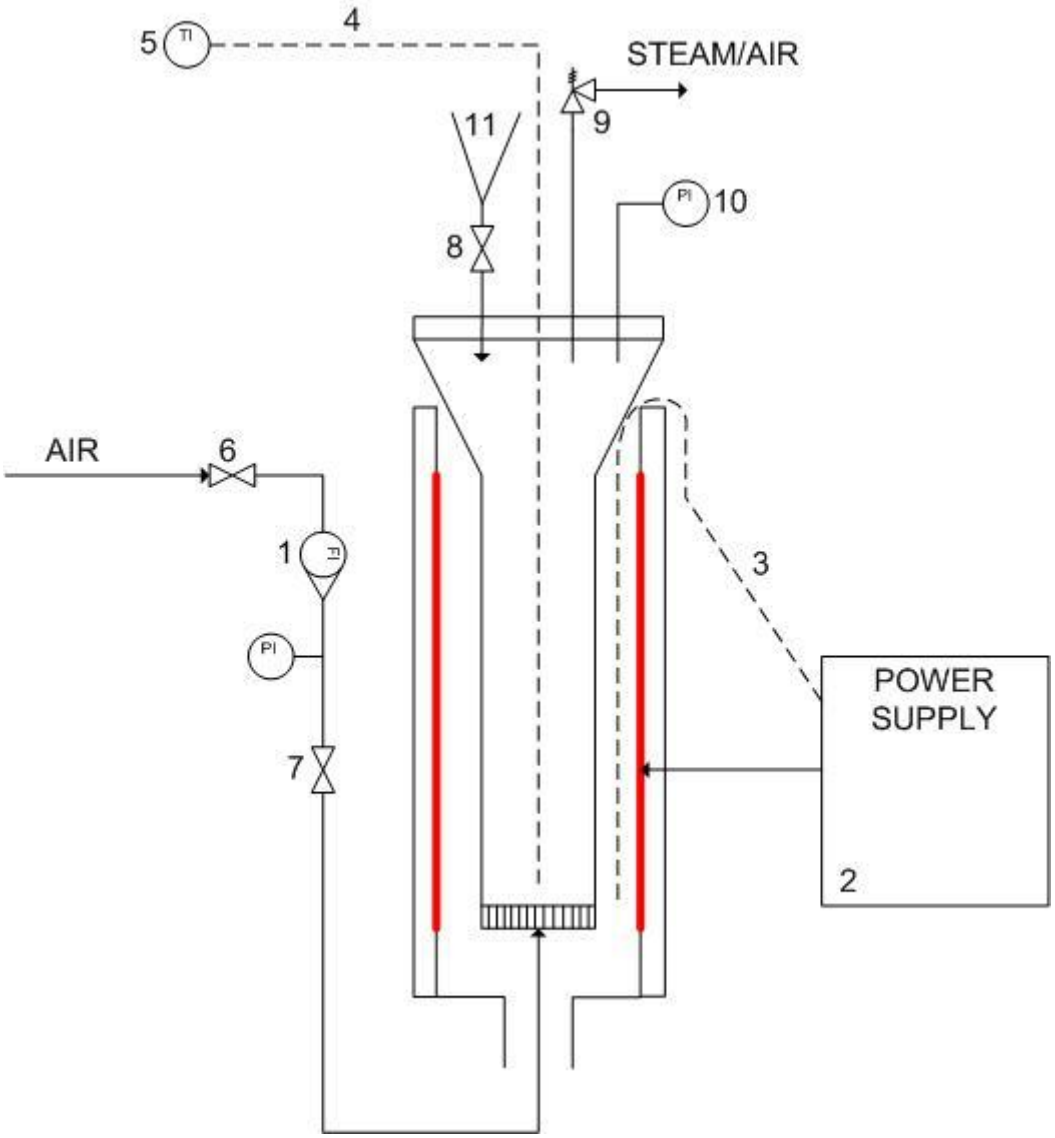

Figure 14. Schematics of the laboratory scale fluidized bed reactor working under pressure. The pieces numbered are: (1) rotameter, (2) power supply, (3) thermocouple measuring the outside temperature of the reactor, (4) thermocouple measuring the inside temperature of the reactor, (5) temperature indicator, (6) air valve, (7) air valve, (8) material feeding valve, (9) pressure relief valve, (10) pressure gauge and (11) material feeding device.

5.2 Other experimental equipment

As mentioned, other equipment was used for cold fluidization tests and analytical work. The cold fluidization apparatus was used for the determination of the minimum fluidization velocity. This ensured the fully turbulent fluidization conditions in the main test apparatus, the fluidized bed reactor. The muffle furnaces were used for the LOI tests, DTA and particle size analysis machines as well as the jet

sieve for additional test work. The X-ray diffractometry machine was located in the University of Auckland in New Zealand and not in Outotec's Frankfurt R&D Center.

5.2.1 The cold fluidization apparatus

The cold fluidization apparatus comprised a 50 mm wide and a 101 cm tall transparent plastic tube with a porous plate in the bottom. At the height of 53 cm the tube had a widening making the rest of the tube 80 mm wide. Air was fed from the instrumental air pipeline through a rotameter, calibrated for carbon dioxide and with a scale of 10 up to 220 l/h, below the porous plate to ensure fluidization. A manometer filled with colored water was connected to the system to measure the bed pressure drop (mmH_2O) of the bed and the porous plate. Figure 15 presents the schematics of the cold fluidization apparatus.

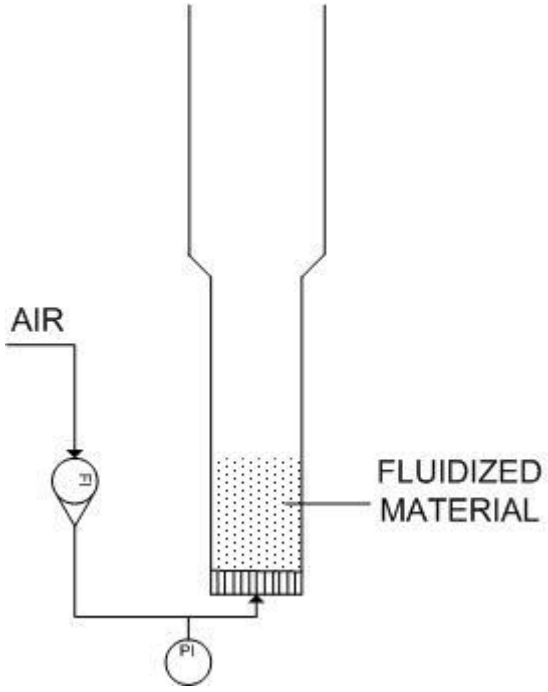

Figure 15. Schematics of the cold fluidization apparatus. The apparatus comprised a 50 mm wide and 101 cm tall transparent plastic tube which had a widening up to 80 mm at a height of 53 cm, a glass rotameter with a scale of 10 to 220 l/h (calibrated for carbon dioxide) and a manometer filled with colored water to measure the pressure loss (mmH_2O) of the porous plate and the bed itself.

5.2.2 Equipment for the analytical work

As mentioned, two different muffle furnaces were used. The first one was a Gerhardt furnace operating at 300 °C for the MOI (Moisture On Ignition, see section 6.2) determination. The other one was a Heraeus furnace for the LOI determination and operated at 1000 °C. Both furnaces were big enough to fir five platinum crucibles inside without problems.

The laser diffraction machine was a Cilas 920 device. Water was used as the carrying liquid. The jet sieve used in this work was an Alpine jet sieve equipped with a 45 µm sieve. The apparatus for the DTA measurements was a Neztsch STA 409. Finally, the X-ray diffractometry was performed with a Brucker D8 using Cu K(α) X-rays.

6 EXPERIMENTAL PROCEDURES

The procedures on how each test was made are presented in this chapter. The calcination procedure is presented in an instructional format due to the fact that formulating a working procedure for the apparatus was one of the goals of the thesis. The instructions give a standard operating procedure for the apparatus and should therefore be followed to receive comparable results. The other procedures explained are the determination of LOI, the cold fluidization test to determine minimum fluidization velocity, particle size analysis in the Cilas machine as well as in the jet sieve, the DTA and the X-ray diffraction tests.

6.1 Calcination procedure

The calcination tests were carried out using sixty grams of dry aluminum trihydroxide. During the test work, three parameters were varied. Six different temperatures: 230, 300, 350, 600, 800 and 900 °C. Several different residence times were also used: 5, 10, 15, 30, 60 and 120 minutes. Moreover, three different pressures were used: 0, 3 and 6 bar over pressure. The fluidization velocity was kept constant in each test. This value only considered the air flow through the reactor and sis not take the accumulating vapor into account.

The first thing is that the rotameter (1) measuring the flow of the air into the reactor is calibrated for oxygen in 40 °C and 201,3 kPa pressure. As the fluidizing

medium is air, comprising a different density, temperature and pressure, the rotameter has to be recalibrated in order to get the new volume flow. This can be done using equation (12). (Rollmann[36], 2008)

$$\dot{V}_{new} = \sqrt{\frac{\rho_1}{\rho_2}} \cdot \sqrt{\frac{P_1}{P_2}} \cdot \sqrt{\frac{T_2}{T_1}} \cdot \dot{V}_{old} \qquad (12)$$

where $\dot{V}_{new,old}$ volume flows, [$m^3 h^{-1}$]
$P_{1,2}$ pressure of the new and old gas, [Pa]
$\rho_{1,2}$ density of the old and new gas, [kg m^{-3}]
$T_{1,2}$ temperature of the old and new gas, [K]

Heating up the reactor is done by switching on the power supply (2) and changing the desired temperature in the display. As the temperature displayed on the power supply is the temperature outside the reactor it is necessary to insert a slightly higher value than what is wanted inside the reactor. The thermocouple (3) should be located in between the reactor and the ceramic plates at this time. It can be placed from the top of the heating tube into the same place as the reactor thus, running aside the reactor. The other thermocouple (4) which measures the inside temperature of the reactor goes through the reactor lid. It should be connected to the temperature meter (5) which can also be switched on at this moment.

After the heating is switched on and the temperature is set the gas flow can be turned on. The valve at the connection between the hose and the air pipeline (6) is opened as well as the valve after the rotameter (7). The hose connecting the valve after the rotameter (7) to the bottom pipe of the reactor has to be securely fastened. The air flow is then set with the rotameter to the value calculated with equation (12). After the air flow is switched on pressure starts accumulating inside the reactor. If atmospheric conditions are desired the feed valve (8) can be opened. If not, the feeding valve should be closed and the pressure relief valve (9) opened. This lets the excess air exit the reactor. The pressure is set by turning the valve either to let more air go through or vice versa. The pressure itself can be observed from the pressure gauge (10). The rotameter must be checked at this point, because the airflow changes when regulating the pressure adjusting valve. After the temperature, air flow and pressure is set the reactor heats up to the desired temperature in approximately thirty minutes to two hours. The crack at the top of the

heating tube between the reactor and the heating tube as well as the bottom of the heating tube can be padded with glass wool to prevent a cool air draft from being in contact with the heating plates and the reactor.

After the reactor has heated up to the desired temperature and has become stable (kept the same temperature for over five minutes) it can be loaded. Usually, it is quite hard to have an exact temperature inside the reactor and therefore a temperature of five degrees either way is acceptable. The amount of the material that is fed into the reactor can basically be anything between ten and a hundred grams. The more the material, the more the inside temperature of the reactor will drop. Fifty to sixty grams is an amount that the reactor temperature does not drop too much making the test work fairly easy. The material is fed into the little bin (11) located above the feeding valve. Before the material is fed the valve (7) after the rotameter must be shut. The material has to be fed into the reactor very quickly due to the fact that if the feeding valve (8) must be closed and the air flow opened immediately. If the feeding valve is not closed quickly enough in high temperatures the steam generated via calcination shoots the material out of the reactor leaving only roughly one third inside the reactor. After this the rotameter (1), temperature meter (5) and the pressure gauge (10) has to be checked. The air flow and the pressure can be adjusted quickly but the temperature takes a longer time. The temperature inside the reactor usually drops over one hundred degrees and has to be heated up as fast as possible. Five minutes or under is enough time to maintain a stable temperature again. The temperature of the heating device should be raised to speed up the heating. Initially, the temperature can be increased roughly 20 °C. If the temperature of the reactor does not start to increase rapidly enough then the temperature can be increased with another 30 °C. When the temperature of the reactor starts to increase, the temperature is lowered again to prevent the reactor from overheating. As mentioned earlier, again a five degree difference in the temperature either way is acceptable. It is important to monitor the pressure and especially the temperature of the reactor when the test is running. The relief valve (9) might become clogged and thus sometimes needs a gentle tap. The temperature on the other hand might not be stable as the calcination is running. This especially the case in the area around 300 and 350 °C because most of the steam is generated in these temperatures. It can be quite difficult to maintain a

stable temperature because the steam cools the reactor down as long as there is steam to be generated. Finally, the temperature may rise rapidly as the generation of steam comes to an end.

When the desired calcination time is two minutes to the end, the reactor temperature is recorded. When the time is up the airflow is shut by closing the air valve (6) and disconnecting the air hose connected to the bottom pipe of the reactor. The power supply (2) is also turned off. The lid of the reactor is opened by unscrewing the nuts that are tightening the bolts. The reactor thermocouple (4) is also disconnected. When the lid is ready to be lifted special attention must be held not to drop moist powder stuck onto the inside of the lid back into the reactor. After the lid is lifted away and the seal is removed the reactor is lifted from the heating device with a crane. The thermocouple measuring the outside temperature of the reactor (3) must be removed at this point. The reactor is lifted and placed into a holder situated next to the heating device. After the reactor is in place the holder is tilted and the powder inside is poured into a bucket. The material is then weighed and placed into a jar and subsequently into a dry place (an exsiccator). The entire operation should take five minutes or under.

The reactor is then cleaned with pressurized air and placed back into the heating device. The thermocouple measuring the reactor outside temperature (3) is put in place just before the reactor is at its final position. The lid seal is put in place. The lid is also cleaned and lifted back on top of reactor. The bolts are connected and the nuts are tightened in a way that each nut is tightened after the opposite one. This ensures an even tightness without leaking. The thermocouple measuring the inside temperature of the reactor (4) and the air hose are finally connected. Finally, it is important to notice that the reactor should be heated in five minutes to a desired temperature after the material is fed. The same five minutes applies when the reactor is lifted out of the heating device and emptied. This means that a fifteen minute test, for example, would take twenty minutes altogether (the heating time is already included into the residence time).

6.1.1 Test work for short residence times

The tests with short residence times (five and ten minutes) were done in atmospheric pressure. This was due to the fact that the use of the crane located above

the fluidized bed reactor was quite time consuming compared to the actual calcination. The entire reactor was therefore lifted by hand out of the heating device. Ten grams of aluminum trihydroxide was used in these tests to ensure that the reactor temperature did not decrease too much. The alumina was then poured directly into a bucket without the use of the apparatus to tilt the reactor. Then the material was stored in metal jars inside an exsiccator. Naturally, due to safety reasons these tests were only done in the lower temperatures (230, 300 and 350 °C).

To realize short residence times, another method was also tested. A cup was welded to the bottom of a narrow pipe. Only roughly two to three grams of aluminum trihydroxide was placed into the cup and a thermocouple was fed into the pipe and eventually into the cup. The cup was then lowered to the bottom of the reactor. The reactor lid could not be used in these tests and therefore the tests were also done in atmospheric pressure. The cup was heated to the desired temperature with a very short residence time. The alumina was weighed and placed into a jar.

6.2 Determining Loss on Ignition

The LOI was determined via an international standard ISO 806:2004(E)[37]. The method is suitable for the measurement of the losses of mass referred as MOI (Moisture On Ignition) and LOI. MOI is the loss of moisture before the sample is ignited. The principle of the test is that the sample is dried at 300 °C for two hours. It is weighed and then ignited at 1000 °C for two hours. Then it is weighed again. MOI and LOI can be calculated from the mass differences.

In this work, five platinum crucibles were used. The crucibles were weighed with an accuracy of 0,0001 g. After this, the five grams (±0,5 g) of alumina was placed into the crucible. The crucibles were placed into the first muffle furnace operating at 300 °C for two hours. After this, the crucibles were taken out and immediately placed into an exsiccator to be cooled down. After the crucibles were cool enough to handle they were weighed and placed into the second muffle furnace operating at 1000 °C. The crucibles were held in the second furnace for two hours and again placed immediately into an exsiccator. After they had cooled down, the samples were weighed again. MOI and LOI were calculated as percentages with the following equations:

$$MOI = \frac{m_2 - m_3}{m_2 - m_1} \cdot 100\% \quad (13)$$

where, m_1 weight of the empty crucible, [g]
m_2 weight of the empty crucible and sample, [g]
m_3 weight of the empty crucible and dried sample, [g]

$$LOI = \frac{m_3 - m_4}{m_2 - m_1} \cdot 100\% \quad (13)$$

where m_4 weight of the empty crucible and ignited sample, [g]

The two values are then added to obtain the final LOI value that indicates the total amount of water (steam) that has left the particle.

6.3 Other test work

Aside the calcination and loss on ignition test work, other tests were performed as well. These included the determination of minimum fluidization velocity, particle size analysis, differential thermal analysis (DTA) and X-ray diffraction (XRD) tests.

6.3.1 Determining the minimum fluidization velocity

The minimum fluidization velocity was determined in the cold fluidization apparatus. One hundred grams of aluminum trihydroxide was placed into the 50 mm pipe which was then fluidized with air. Due to the fact that the rotameter was calibrated for carbon dioxide it had to be recalibrated for air. Initially, the rotameter showed a flow of 0 l/h. This was then increased to 120 l/h by 10 l/h intervals. After 120 l/h the flow was raised with intervals of 20 l/h up to 220 l/h. These values then had to be converted for air. After the maximum value was reached, the value was lowered to 0 l/h with the same intervals. This test was then duplicated. Naturally, the pressure drop for the porous plate alone had to be measured to determine the pressure drop caused only by the bed.

After each increase in the flow the pressure drop of the porous plate and the bed was measured. The measurement was done with a manometer filled with colored water (mmH_2O). The pressure drops were then recorded. The fluidization velocity

was calculated from the gas volume flow and the area of the fluidization tube. Furthermore, the minimum fluidization velocity was determined from the crossing of the rising section of the pressure drop and the horizontal section as presented in figure 11.

6.3.3 Particle size analysis

A particle size analysis was done with a Cilas 920 laser diffraction device to see the effect of pressure to the mean particle size. Approximately one gram was weighed into the machine where water the carrying medium. The particle size distribution as well as the mean particle size was calculated by the computer and printed out as a sheet.

Because about 92 % of the produced alumina sent for the electrolyte smelters has to have a particle size over 45 µm (Hudson *et al*[1], 2000), the pressure calcined alumina was tested for this. Roughly fifteen grams of alumina was placed onto the jet sieve equipped with a 45 µm sieve. The sieve was turned on for six minutes. Air was sucked through the sieve leaving the coarse particles on top and removing the fine particles into a dust container. The remaining amount of alumina was then collected from the sieve and weighed. Due to the fact that alumina has a strong affinity for water the same jet sieve test was done after letting the alumina air calibrate in room temperature in a large ceramic bowl for twelve hours.

6.3.3 Differential thermal analysis

The differential analysis was done by measuring fifty milligrams of aluminum trihydroxide into the sample holder. The inert reference sample was alumina. The tests were made with an airflow of <50 ml/h and 200 ml/h to demonstrate the possible effect of partial steam pressure. The aim was that when increasing the air flow, the partial pressure of steam would decrease leading to lower water content than when using an air flow of <50 ml/h. The tests were made with a temperature increase of 10 °C per minute from a minimum of room temperature (roughly 20 °C) up to a maximum of 1000 °C.

6.3.4 X-ray diffraction

The XRD tests were made for the samples calcined with a six bar over pressure and sixty minutes residence time to determine the effect of pressure to the route of the thermal decomposition of aluminum trihydroxide. The calcination temperatures for the samples were: 230, 300, 350, 600, 900 °C. Also, one sample calcined in atmospheric pressure and 900 °C with 60 minutes residence time was characterized. The tests were performed by Mr. Linus Perander in the University of Auckland (New Zealand). The analysis was performed with a 2θ angle of 10-80°, a step width of 0,02° and a counting time of 10 seconds. A Rietveld refinement for the X-ray diffractograms was performed using the FullProf[38] software package. Furthermore, Mr. Linus Perander interpreted the results into a report format, Perander[39] (2008).

10 REFERENCES

1 Hudson, L., Misra, C., Perrotta, A., Wefers, K., Williams F., Aluminum oxide, Ullmann's encyclopedia of industrial chemistry, Wiley & Sons, 2000

2 Slade, R.C.T., Southern, J.C. and Thompson, I.M., 27Al nuclear magnetic resonance spectroscopy investigating of thermal transformation sequences of alumina hydrates Part 1. – gibbsite γ-Al(OH)3, Journal of materials chemistry, 1(4), 1991, p.563-568,

3 Wefers, K., Misra, C., Oxides and hydroxides of aluminium, Alcoa Technical Paper 19, 1987

4 Paglia, G., Bucley, C.E., Rohl, A.L., Hart, R.D., Winter, K., Studer A.J., Hunter, B.A., Hanna, J.V., Boehmite Derived γ-Alumina System. 1. Structural Evolution with Temperature, with the Identification and Structural Determination of a New Transition Phase, γ'-Alumina, Chem. Mater., 16, 2004, p. 220-236

5 Gan, B.K., Crystallographic transformations involved in the decomposition of gibbsite to alpha alumina, PhD thesis, Curtin University of Technology, Australia, 1996

6 Klett, C., Missalla, M., Bligh, R., Ströder, M., Hiltunen, P., Graham, M., Outokumpu Technology's State-of-the-Art CFB Calciners – A Review, Proceedings of EMC, 2007

7 Ullmann's Encyklopädie der technischen Chemie, Vol. 7, Acaricide bis Antihistaminica, Verlag Chemie GmbH, Weinheim/Bergstr., 1973, p. 318

8 HSC Chemistry 5.11, Outokumpu Research Oy, Outokumpu Technologies

9 Zwicker, J. D., The generation of fines due to heating of alumina trihydrate, Light Metals, 1985, p. 377-396

10 Zivkovic, Z.D., Filipovic, M., Change of granulometric composition during calcination of aluminum hydroxide, International Etude Bauxites, Alumine Alum., 16, 1981, p. 383-389

11 Ollivier, B., Retoux, R., Lacorre, P., Massiot, D., Ferey, G., Crystal structure of κ-alumina: and X-ray powder diffraction, TEM and NMR study, Journal of Material Chemistry, **7**, 1997, p. 1049-1056

12 Naumann, R., Kohnke, K., Paulik, J., Paulik, F., Kinetics and me chanisms of the dehydration of hydragillites Part II, Thermochimica Acta, 64, 1983, p. 15-26

13 De Boer, J.H., Fortuin J.M.H., Steggerda, J.J., The dehydration of alumina hydrates, Proc. Kon. Ned. Akad. Wetensch, Amsterdam, B57, 9, 1953, 170-180

14 Ingram-Jones, V.J., Slade, R.C.T., Davies T.W., Southern J.C., Sal vador, S., Dehydroxylation sequences of gibbsite and boehmite: study of differences between soak and flash calcination and of particle size effects, Journal of Materials Chemistry, 6, 1996, p. 73-79

15 Whittington, B., Ilievski, D., Determination of the dehydration reaction pathway at conditions relevant to Bayer refineries, Chemical Engineering Journal, 98, 2004, p. 89-97

16 Yamada, K., Harato, T., Hamano, S., Horinouchi, K., Dehydration products of gibbsite in rotary kiln and stational calciner, Light Metals, 1984, p.157-171

17 Roquerol, J., Roquerol, F., Ganteaume, M., Thermal decomposition of gibbsite under low pressures I. Formation of boehmitic phase, Journal of Catalysis, 36, 1975, p. 99-110

18 Sucech, S. W., Misra, C., Alcoa pressure calcination process for alumina, Light Metals, 2, 1986, p. 119-124

19 Perry's chemical engineer's handbook, Perry, R.H., 7th Ed., McGraw-Hill, 1997

20 Geldart, D., Gas fluidization technology, John Wiley & Sons, 1986

21 Kunii, D., Levenspiel, O. Fluidization Engineering, Butterworth-Heinemann, 1991

22 Introduction to some particle technology phenomena, available at [18.6.2008]: http://users.monash.edu.au/~rhodes/education.htm

23 Ergun, S., Fluid flow through packed bed columns, Chemical Engineering Progress, 48, 1954, p. 89-94

24 Wen, C.Y., Yu, Y.H., Mechanics of fluidization, Chemical Engineering Progress Symposium Series, 62, 1966, p. 100

25 Delebarre, A. Revisiting the Wen and Yu equations for minimum fluidization velocity prediction, Chemical engineering research and design, 82(A5), 2004, p. 587-590

26 Rowe, P. N., The effect of pressure on minimum fluidization velocity, Chemical Engineering Science, 39, 1984, p. 173-174

27 King, D.F. and Harrison, D.L., The dense phase of a fluidized bed at elevated pressures, Chemical engineering research and design, 60, 1982, p. 20-30

28 Yates, J. G., Effects of temperature and pressure on gas-solid fluidization, Chemical engineering science, Vol. 51 No. 2, p.167-205, 1996

29 Niro Inc. Fluidized bed drying – fundamentals. Available at [7.5.2008]:http://www.niroinc.com/drying_dairy_food/fluid_bed_technology.asp

30 Outotec's calcination plant process description, given by Mr. Michael Missalla, 12.3.2008

31 Reh L., Challenges of circulating fluid-bed reactorsin energy and raw material industries, Chemical Engineering Science, 54, 1999, p. 5359-5368

32 Yang, W-C., Circulating fluidized beds, Handbook of Fluidization and Fluid-Particle Systems, Marcel Dekker, 2003

33 Yang, W-C., Particle characterization and dynamics, Handbook of Fluidization and Fluid-Particle Systems, Marcel Dekker, 2003

34 Lurgi sheet comparing stationary and circulating fluidized beds, Stationary and fast fluid beds, given by Mr. Andreas Spies, 24.4.2008

35 Melnikowitsch, D., Master of Science Thesis, Outotec GmbH R&D Center Frankfurt, 2008

36 Rollmann, G., Calculation of correction factors for variable area flow meters at deviating working conditions, available at [17.6.2008]: http://www.ktweb.de/pdf/physik/korrekturfaktorenberechnung_gb_2.2.pdf

37 ISO Standard, ISO806:2004(E), Aluminium oxide primarily used for the production of aluminium – Determination of loss of mass at 300 °C and 1000 °C, 2nd Ed.

38 Rodriguez-Carvajal, J., FULLPROF: A program for Rietveld Refinement and pattern matching analysis. In abstracts of the satellite meeting on powder diffraction of the XV Congress of the IUCr, Tolouse, France, 1990

39 Perander, L., Characterization of alumina samples prepared under pressurized calcination conditions, Light Metals Research Center, 2008